ARTHRITIS & RHEUMATISM
Vol. 65, No. 11, November 2013, pp 2928–2939
DOI 10.1002/art.38078

Endothelial Injury in a Transforming Growth Factor β–Dependent Mouse Model of Scleroderma Induces Pulmonary Arterial Hypertension

Emma C. Derrett-Smith,[1] Audrey Dooley,[1] Adrian J. Gilbane,[1] Sarah L. Trinder,[1] Korsa Khan,[1] Reshma Baliga,[2] Alan M. Holmes,[1] Adrian J. Hobbs,[2] David Abraham,[1] and Christopher P. Denton[1]

Objective. **To delineate the constitutive pulmonary vascular phenotype of the TβRIIΔk-fib mouse model of scleroderma, and to selectively induce pulmonary endothelial cell injury using vascular endothelial growth factor (VEGF) inhibition to develop a model with features characteristic of pulmonary arterial hypertension (PAH).**

Methods. **The TβRIIΔk-fib mouse strain expresses a kinase-deficient transforming growth factor β (TGFβ) receptor type II driven by a fibroblast-specific promoter, leading to ligand-dependent up-regulation of TGFβ signaling, and replicates key fibrotic features of scleroderma. Structural, biochemical, and functional assessments of pulmonary vessels, including in vivo hemodynamic studies, were performed before and following VEGF inhibition, which induced pulmonary endothelial cell apoptosis. These assessments included biochemical analysis of the TGFβ and VEGF signaling axes in tissue sections and explanted smooth muscle cells.**

Results. **In the TβRIIΔk-fib mouse strain, a constitutive pulmonary vasculopathy with medial thickening, a perivascular proliferating chronic inflammatory cell infiltrate, and mildly elevated pulmonary artery pressure resembled the well-described chronic hypoxia model of pulmonary hypertension. Following administration of SU5416, the pulmonary vascular phenotype was more florid, with pulmonary arteriolar luminal obliteration by apoptosis-resistant proliferating endothelial cells. These changes resulted in right ventricular hypertrophy, confirming hemodynamically significant PAH. Altered expression of TGFβ and VEGF ligand and receptor was consistent with a scleroderma phenotype.**

Conclusion. **In this study, we replicated key features of systemic sclerosis–related PAH in a mouse model. Our results suggest that pulmonary endothelial cell injury in a genetically susceptible mouse strain triggers this complication and support the underlying role of functional interplay between TGFβ and VEGF, which provides insight into the pathogenesis of this disease.**

Pulmonary arterial hypertension (PAH) develops in up to 10% of patients with systemic sclerosis (SSc; scleroderma) and is a major cause of mortality (1,2). The worse outcomes and poorer responses to therapy in patients with SSc-related PAH compared with idiopathic PAH suggest that clinical and pathologic differences exist between different forms of precapillary pulmonary hypertension (3). In SSc, the timing and frequency of the development of PAH are consistent with a triggering event in susceptible individuals (4). The pathologic hallmark of advanced SSc-related PAH is vascular obliteration with endothelial proliferation, medial hypertrophy, and adventitial fibrosis. Endothelial injury and

Supported by Arthritis Research UK (grants 17982, 19700, and 19427), the Scleroderma Research Foundation, and the British Heart Foundation.

[1]Emma C. Derrett-Smith, PhD, MRCP, Audrey Dooley, PhD, Adrian J. Gilbane, MSc, Sarah L. Trinder, PhD, Korsa Khan, BSc, Alan M. Holmes, PhD, David Abraham, PhD, Christopher P. Denton, PhD, FRCP: University College London Medical School, Royal Free Campus, London, UK; [2]Reshma Baliga, PhD, Adrian J. Hobbs, PhD: William Harvey Research Institute and Barts and the London School of Medicine and Dentistry, Queen Mary, University of London, London, UK.

Dr. Hobbs has received consulting fees, speaking fees, and/or honoraria from Bayer AG, Novartis, and Palatin Technologies (less than $10,000 each).

Address correspondence to Christopher P. Denton, PhD, FRCP, Centre for Rheumatology and Connective Tissue Diseases, University College London Medical School, Royal Free Campus, Rowland Hill Street, London NW3 2PF, UK. E-mail: c.denton@ucl.ac.uk.

Submitted for publication October 3, 2012; accepted in revised form June 27, 2013.

apoptosis have been reported, and perivascular inflammation has been observed (5–9).

Dysregulated angiogenesis, with high levels of circulating vascular endothelial growth factor (VEGF) and angiostatic factors, is thought to represent an aberrant repair mechanism (10,11). These changes are present in the arterial circulation of patients with other forms of PAH, but pulmonary vascular changes may be more widespread in SSc and involve the pulmonary venous network (12,13); this may, in part, underlie the clinical differences in mortality and response to therapy in SSc-related PAH.

Genetic susceptibility to PAH in patients with SSc has not yet been clearly shown. Although no association has been observed with the gene encoding bone morphogenetic protein receptor type II, which underlies some heritable PAH and idiopathic PAH (14), a role for altered transforming growth factor β (TGFβ) superfamily signaling remains possible. Recent studies have revealed polymorphisms in the endoglin gene (an accessory receptor for TGFβ ligand that has been shown to be altered in SSc) and *KCNA5* in other forms of PAH (15,16).

In this study, we replicated hallmark features of PAH by administering the VEGF receptor inhibitor SU5416 to TβRIIΔk-fib mice, which have previously been shown to develop several features of human scleroderma. We demonstrate a constitutive pulmonary vascular phenotype reminiscent of the murine chronic hypoxia model of pulmonary hypertension (PH), including changes in medial hypertrophy and raised pulmonary arterial pressure. We show that administration of SU5416 induces obliterative endothelial proliferation characteristic of SSc-related PAH, thus providing insight into the pathogenesis of SSc-related PAH and generating a novel mouse model of potential value in preclinical studies of therapies for this important complication of SSc.

MATERIALS AND METHODS

Generation of TβRIIΔk-fib–transgenic mice. The generation of TβRIIΔk-fib–transgenic mice has been described previously (17,18). Mice were genotyped by polymerase chain reaction, using primers specific to LacZ and an internal control. Each experiment was performed by comparing at least 6 mice for each condition and sex-matched littermate controls, and then the experiments were performed in triplicate. Mice were ages 6–8 weeks in all of the experiments except the hemodynamics experiments, in which (for technical reasons) the mice were ages 12 weeks. Measurements were made by observers blinded to treatment category or genotype. A 50-mg/kg intraperitoneal injection of SU5416 (Sigma) in carboxymethylcellulose vehicle was administered, as previously described (19,20). The mice were housed in a clean conventional colony, with access to food and water ad libitum. Strict adherence to institutional guidelines was practiced, and full local ethics committee and Home Office approval were obtained prior to all animal procedures.

Long-term exposure to hypoxia. Mice undergoing exposure to hypoxic conditions were housed in a normobaric hypoxia chamber (850-NBB Nitrogen Dry Box; Plas-Labs) for 3 weeks. Room air balanced with N_2 achieved an FiO_2 value of 0.10. CO_2-absorbent lime was added to maintain the CO_2 content at $<1.0\%$. Gas tension and humidity values were determined daily to ensure optimal conditions.

Histologic analysis. Lung and cardiac tissue specimens were immersed in 10% formal saline, gluteraldehyde, RNAlater (Ambion), or liquid nitrogen. Formalin-fixed, paraffin-embedded sections were stained with hematoxylin and eosin (H&E), picrosirius red, or elastic–van Gieson for immunohistochemical analysis, as previously described (21). The primary antibodies were β-galactosidase, CD31, VEGF, VEGF receptor 1 (VEGFR-1), VEGFR-2, CD3, CD19, and CD68 (Abcam), TGFβ1 and p-Smad2/3 (Santa Cruz Biotechnology), latency-associated peptide (LAP) TGFβ1 (R&D Systems), α-smooth muscle actin (Sigma-Aldrich), Ki-67 (Dako), and cleaved caspase 3 (Cell Signaling Technology). Sections were viewed and measurements quantified with an Axioskop Mot Plus microscope using AxioVision software (Zeiss). Vessel thickness was measured using the first 10 consecutive H&E-stained sections of the right lung, comprising both proximal and distal vessels in each case. Vessels that had been sectioned obliquely or longitudinally were not included in the analysis. Sections used for transmission electron microscopy were stained with uranyl acetate and Reynold's lead citrate and viewed using a Philips 201 transmission electron microscope. Colocalization was demonstrated by immunostaining, using multichannel immunofluorescence microscopy.

In vivo measurement of right ventricular systolic pressure (RVSP) and hypertrophy. Hemodynamic measurements of RVSP and mean arterial blood pressure were obtained in 12-week-old male TβRIIΔk-fib mice and wild-type (WT) littermate mice (20–25 gm). The mice were anesthetized with 1.5% isoflurane and placed in a supine position onto a heating blanket that was thermostatically controlled at 37°C. First, the right jugular vein was isolated, and a Millar SPR-671NR mouse pressure catheter with a diameter of 1.4F was introduced and advanced into the right ventricle to determine RVSP. Next, mean arterial blood pressure was measured by isolating the left common carotid artery and introducing a pressure catheter. Both RVSP and mean arterial blood pressure measurements were recorded into a precalibrated PowerLab System (ADInstruments). The mice were killed by isoflurane anesthetic overdose, whole blood samples were collected, the hearts were removed, and the weights of the right and left ventricles were recorded.

Quantitative assessment of TGFβ1 in serum and bronchoalveolar lavage (BAL) fluid. Total and free murine TGFβ1 was quantified in serum and BAL fluid using a conventional indirect competitive enzyme-linked immunosorbent assay according to the manufacturer's instructions (R&D Systems). The results were recorded using a Mithras LB 940 Microplate Reader.

Primary pulmonary artery smooth muscle cell (PASMC) culture, analysis, and staining. En bloc mouse heart and lung was microdissected in Hanks' balanced salt solution. The pulmonary artery was identified from its origin in the right ventricle and followed to division and entry into the lungs. Surrounding fat and connective tissue were stripped, and the vessel was opened longitudinally. Collagenase digestion was performed before explanting. After 24 hours, the fetal calf serum concentration was reduced from 10% to 0.2%. For cell hypoxia experiments, PASMCs were plated in separate 6-well plates. The cells were serum-starved and treated with recombinant TGFβ1 (4 ng/ml). One plate was incubated in atmospheric oxygen conditions (labeled 21%), and the paired plate was incubated inside a modular incubator chamber (Billups-Rothenburg) containing humidified hypoxic gas (1% O_2, 5% CO_2 in nitrogen) for 24 hours. Human PASMCs (PromoCell) were cultured in standard conditions, as described above, before lysis for Western blotting.

Cells were seeded for staining in chamber slides (BD Bioscience), fixed with cold methanol, and permeabilized with 0.2% Triton in phosphate buffered saline before blocking with isotype-matched serum for 30 minutes. The cells were then stained for 1 hour with anti–α-SMA or anti–β-galactosidase at 1:100 dilution, washed, and incubated with the appropriate conjugated secondary antibody (Vector BioLabs) before washing and mounting with Vectastain, and examined with an Axioskop Z Fluorescence Microscope (Zeiss).

Aortic smooth muscle cell (SMC) culture. The aortae were dissected, the adventitia stripped, and the vessel opened longitudinally. After collagenase digestion (1 mg/ml) for 10 minutes at 37°C to remove the endothelium, the remaining SMCs were grown by explant culture as described above for PASMCs.

RNA quantitation and analysis. Total RNA was extracted, quantified, and subjected to quantitative reverse transcription–polymerase chain reaction analysis, as described previously (22). The minimum 260:280 ratio was 1.88. RNA integrity values ranged from 9.1 to 10. The reference genes *Sdha*, *Rpl13*, *ActB*, and *Ubc* were used to compute a normalization factor (23). The primer sequences for the genes of interest were as follows: for mouse *Vegf*, forward 5′-CATCTTCAAGCCGTCCTGTGT-3′ and reverse 5′-CTCCAGGGCTTCATCGTTACA-3′ (assay efficiency 0.92; $R^2 = 0.990$); for mouse *Vegfr-a*, forward 5′-ACTGGACCCTGGCTTTACTG-3′ and reverse 5′-TCTGCTCTCCTTCTGTCGTG-3′ (assay efficiency 0.90; $R^2 = 0.999$).

Western blotting. Human PASMCs were lysed, homogenized with radioimmunoprecipitation assay buffer (Sigma), and stored at −70°C. Protein was fractionated by sodium dodecyl sulfate–polyacrylamide gel electrophoresis using Tris glycine gels (Invitrogen) with a reference ladder (SeeBlue Plus; Invitrogen), at 125V for 1.5–2 hours in Tris/glycine running buffer (Bio-Rad), according to departmental protocols, and electroblotted to nitrocellulose membranes (Hybond-C; Amersham). Nonspecific binding was blocked by membrane incubation with 5% nonfat dry milk in Tris buffered saline–0.1% Tween 20 (Sigma) and incubated with a 1:1,000 dilution of primary antibodies (VEGF, VEGFR-1, and VEGFR-2; Abcam). Blots were then developed by incubation with biotinylated anti-rabbit or anti-mouse antibodies (1:1,000; Vector BioLabs) as secondary antibodies, followed by incubation with Vectastain ABC reagent (Vector BioLabs). Signal was detected using an Amersham ECL luminescence detection kit followed by exposure to photographic film (Hyperfilm ECL; Amersham). Densitometry was performed using Mikro Win 2000 software.

Statistical analysis. Except where indicated otherwise, data are presented as the mean ± SEM of n observations. Statistical analysis was performed using Student's *t*-test or analysis of variance with post hoc correction for pairwise comparisons, using Minitab software. *P* values less than 0.05 were considered significant.

RESULTS

Development of features characteristic of pulmonary vascular disease in TβRIIΔk-fib–transgenic mice. In addition to the development of interstitial fibrosis in a minority of mice at 16 weeks of age (21), TβRIIΔk-fib mice consistently develop a structural pulmonary vasculopathy, as shown in Figure 1. H&E staining of the pulmonary vasculature at low (Figure 1A) and high (Figure 1B) power showed medial thickening and a perivascular inflammatory cell infiltrate (Figure 1A), with increased deposition of extracellular matrix around vascular structures. Picrosirius red staining confirmed increased perivascular collagen deposition, and elastic–van Gieson staining revealed some architectural disruption of elastin in the larger pulmonary artery vessels (Figures 1C and D). Immunostaining with α-SMA was localized to the smooth muscle layer (Figure 1E).

Quantification of inflammatory cellular infiltrates and pulmonary vessel wall thickening was performed. Cell counts performed on high-power field (hpf) images containing a central pulmonary vessel showed higher cell numbers in transgenic mice (mean ± SEM 176 ± 9 nuclei/hpf in transgenic mice and 129 ± 9 nuclei/hpf in WT mice; $P < 0.008$). Immunophenotyping confirmed a proliferating (Ki-67 positive) chronic inflammatory infiltrate containing CD3+ and CD19+ lymphocytes and CD68+ macrophages (Figure 1F).

Vessel wall thickness was expressed as a ratio to the internal circumference of each vessel. Transgenic mice had thicker vessel walls overall, but particularly in the smaller arterioles (diameter 30–60 μm) (Figure 1G). Examination of α-SMA–immunostained samples confirmed that the increased vessel wall diameter in transgenic mice was attributable to increased thickness of the vascular SMC layer (mean ± SEM ratios 0.21 ± 0.01 in transgenic mice and 0.14 ± 0.01 in WT mice; $P < 0.001$). Lung tissue from transgenic mice also showed muscularization in very small vessels, with a mean ± SEM of 3.0 ± 0.99 vessels of <20 μm in diameter/hpf containing

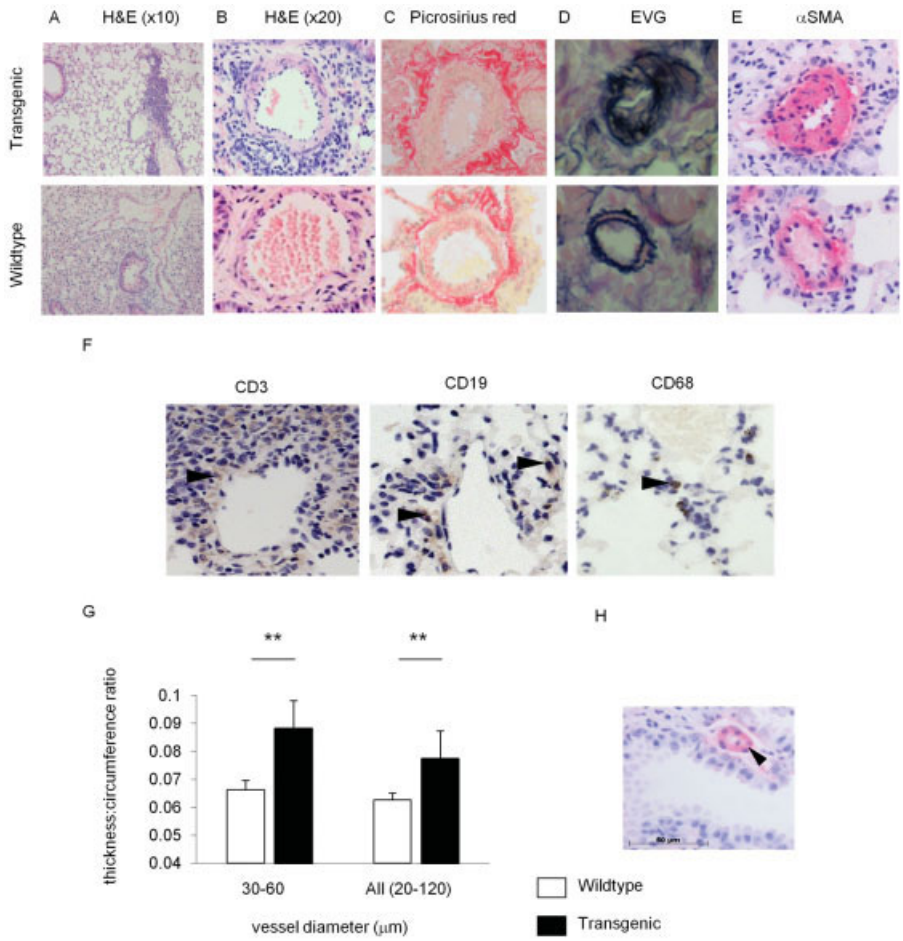

Figure 1. TβRIIΔk-fib–transgenic mice develop characteristic features of pulmonary vascular disease. **A–E,** Representative pulmonary arteriole sections from transgenic and wild-type mice, stained with hematoxylin and eosin (H&E) (**A** and **B**), picrosirius red (**C**), elastic–van Gieson (EVG) (**D**), and α-smooth muscle actin (α-SMA) (**E**). **F,** Immunohistochemical staining of perivascular infiltrate for T cells, B cells, and macrophages from transgenic mice (**arrowheads**). **G,** Pulmonary vessel wall thickness:circumference ratios in wild-type and transgenic mice. Bars show the mean $\pm$ SEM of 1,000 pulmonary vessels. ** = $P < 0.01$. **H,** Muscularization of very small pulmonary vessels in the TβRIIΔk-fib mouse strain (**arrowhead**). Original magnification $\times$ 10 in **A**; $\times$ 20 in **B–E**; $\times$ 20 in **F**; $\times$ 40 in **H**.

α-SMA compared with 1.8 $\pm$ 0.93 of such vessels in tissue from WT mice ($P < 0.05$) (Figure 1H). Other hallmark features of advanced SSc-related PAH, such as intravascular thrombus or plexiform lesions, were not observed. No features suggestive of endothelial proliferation or apoptosis were evident. An examination of endothelial ultrastructure by transmission electron microscopy showed no evidence of endothelial membrane abnormalities (data not shown), in contrast to the alveolar epithelium in the same model (21).

A modest elevation of RVSP was consistently observed in the transgenic mouse strain compared with their WT littermates (for transgenic mice, mean $\pm$ SEM 24.4 $\pm$ 2.6 mm Hg; for WT mice, 18.1 $\pm$ 1.3 mm Hg; $P <$ 0.05). There was no difference in the RV mass index (Fulton index) between transgenic and WT mice.

Alteration of TGFβ expression and signaling within the pulmonary vasculature of TβRIIΔk-fib mice. Consistent with the phenotype of up-regulated TGFβ signaling in fibroblasts and increased TGFβ bioactivity, immunostaining for LAP TGFβ1 and TGFβ1 was increased in the perivascular adventitia of transgenic mice (Figures 2A and B). In transgenic mice, nuclear translocation of p-Smad2/3 was increased in the pulmonary vessels in both the adventitial and smooth muscle layers (Figure 2C). BAL fluid from transgenic mice contained higher total TGFβ compared with that from WT mice (Figure 2D), despite normal serum TGFβ levels (data

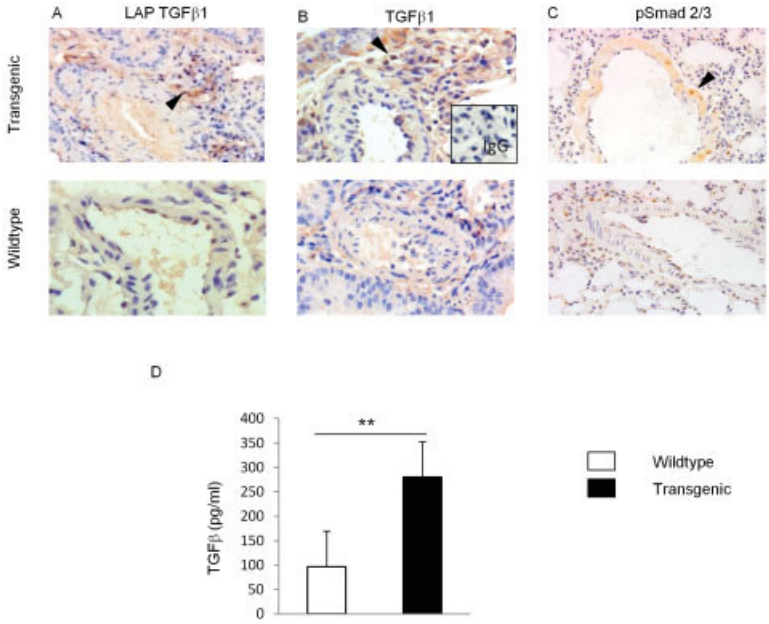

Figure 2. Transforming growth factor β (TGFβ) axis signaling is altered within the pulmonary vasculature of TβRIIΔk-fib mice. **A–C,** Representative images showing latency-associated peptide (LAP) transforming growth factor β1 (TGFβ1), TGFβ1, and p-Smad2/3 immunostaining of pulmonary arteriole sections from transgenic and wild-type mice. Boxed area shows IgG control. **Arrowheads** indicate areas of positive staining. Original magnification $\times$ 20. **D,** Total TGFβ levels in the bronchoalveolar lavage fluid of transgenic mice and their wild-type littermates. Bars show the mean $\pm$ SEM. ** = $P < 0.01$.

not shown). These findings suggested that the increased TGFβ bioavailability and up-regulation of canonical TGFβ signaling in the skin and lungs of transgenic mice also have effects on vascular SMCs that do not express the transgene. The same findings were observed within the aortic SMCs, as previously reported (22).

Pulmonary vascular responses to hypoxia in TβRIIΔk-fib mice. Based on the findings described above, WT and transgenic mice were exposed to hypoxic conditions for 3 weeks and compared with sex-matched littermates kept in room air. These groups were identified as transgenic hypoxic, WT hypoxic, transgenic nor-

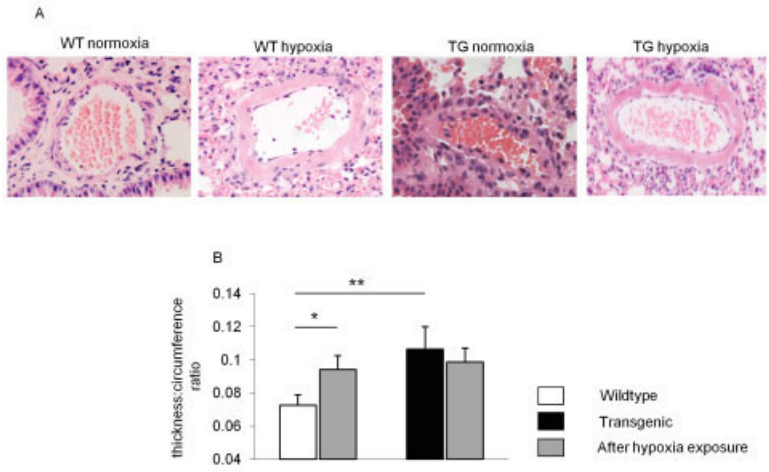

Figure 3. Pulmonary vascular response to hypoxia in the TβRIIΔk-fib mouse strain. **A,** Representative images of hematoxylin and eosin–stained pulmonary vascular wall sections from wild-type (WT) and transgenic (TG) mice exposed to hypoxia and control mice exposed to normoxic conditions. Original magnification $\times$ 20. **B,** Vessel wall thickness:circumference ratio in WT and transgenic mice before and after exposure to hypoxia. Bars show the mean $\pm$ SEM. * = $P < 0.05$; ** = $P < 0.01$.

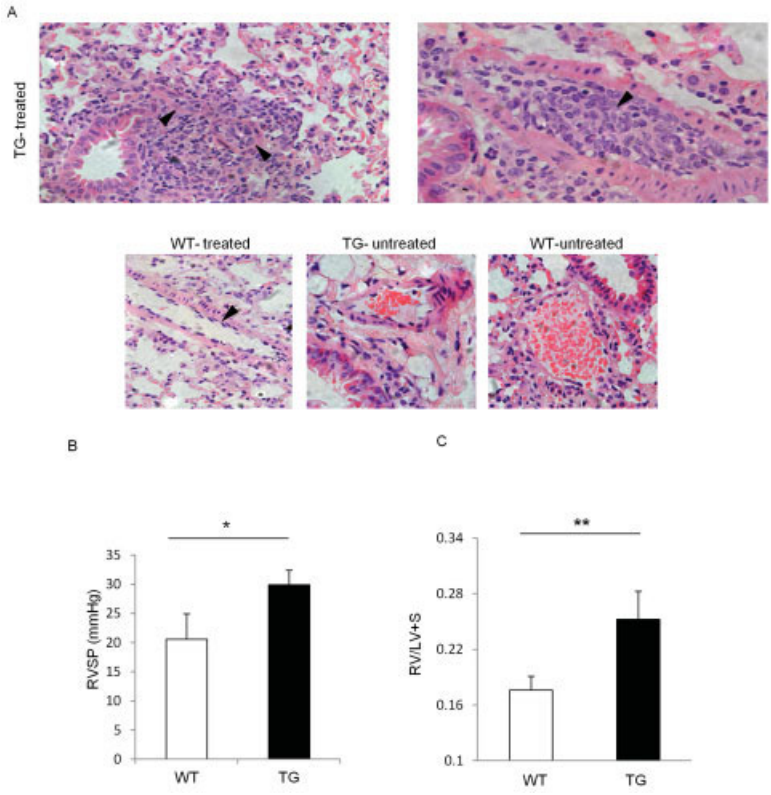

Figure 4. Systemic vascular endothelial growth factor receptor inhibition causes pulmonary arterial hypertension in TβRIIΔk-fib mice. **A,** Representative images of hematoxylin and eosin–stained pulmonary arteriole sections from transgenic (TG) and wild-type (WT) mice treated with SU5416 (S) or left untreated. **Arrowheads** indicate areas of endothelial proliferation. Original magnification × 20. **B** and **C,** Right ventricular systolic pressure (RVSP) (**B**) and RV mass index (**C**) in WT and transgenic mice following treatment with SU5416. Bars show the mean ± SEM of 3 independent replicate experiments. * = $P < 0.05$; ** = $P < 0.01$. LV = left ventricular.

moxic, and WT normoxic. All hypoxic mice lost weight initially, which was regained by 3 weeks, indicating that hypoxia was tolerated well.

The increased thickness:circumference ratio of pulmonary arterioles seen in the transgenic normoxic group was not further exacerbated by hypoxia; hypoxia consistently increased the thickness:circumference ratio compared with normoxia in WT mice (Figure 3B). Hence, the transgenic normoxic mice had vessel wall thickness comparable with that in the WT hypoxic group but were refractory to further medial changes (Figure 3A). Following this period of hypoxia, some mice were returned to normoxic conditions for 4 weeks. The SMC changes present in WT hypoxic mice resolved, and no further histologic change was observed in the transgenic mice. These data suggested that although the constitutive pulmonary vascular phenotype of the TβRIIΔk-fib mouse strain replicates some of the structural features of hypoxic PH in WT mice, it is a persistent phenotype that is not further altered by hypoxia, unlike the reversible structural and hemodynamic hypoxic phenotype seen in WT mice.

Systemic VEGFR inhibition–induced proliferative pulmonary vasculopathy in TβRIIΔk-fib mice. The results of previous studies suggest that endothelial injury using the small molecule tyrosine kinase inhibitor SU5416 may induce obliterative pulmonary vasculopathy in rodents after long-term exposure to hypoxia (19,20). Given the structural and hemodynamic similarities between the constitutive TβRIIΔk-fib mouse pulmonary vascular phenotype and the chronic hypoxia model, including medial hypertrophy without endothelial change and raised pulmonary artery pressure, we induced endothelial injury by administering SU5416 to TβRIIΔk-fib mice. A single intraperitoneal injection of SU5416 was sufficient to induce typical pathologic changes, without exposure to an hypoxic environment. Adult mice ages 6 weeks were used for this experiment

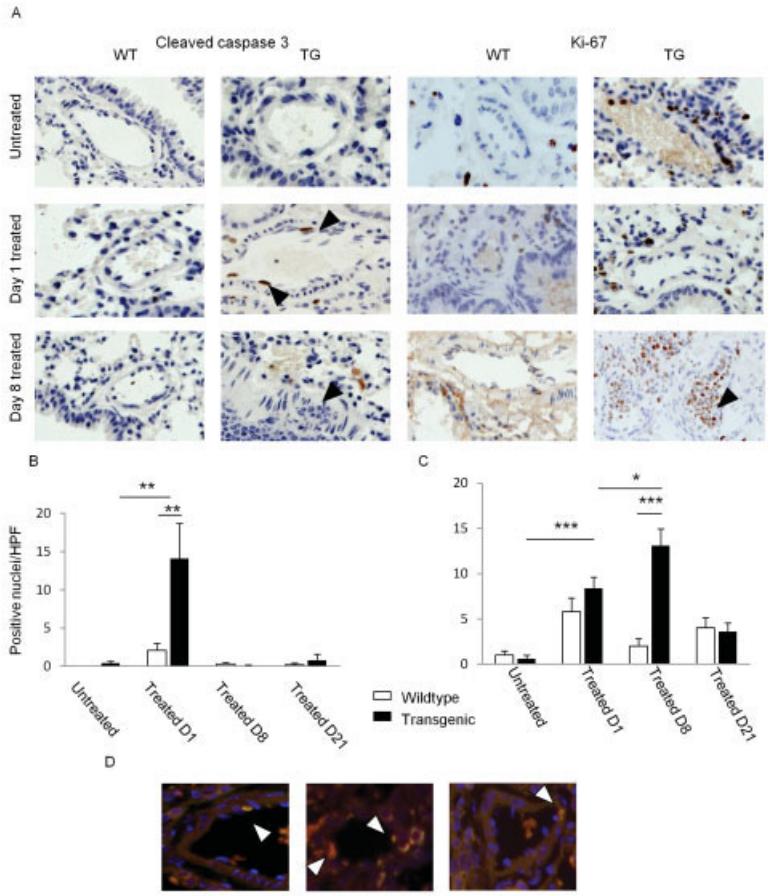

Figure 5. SU5416-induced endothelial cell apoptosis and proliferation in the pulmonary vessels of TβRIIΔk-fib mice. **A,** Representative images showing cleaved caspase 3 and Ki-67 immunostaining of intrapulmonary arteriole sections from wild-type (WT) and transgenic (TG) mice before treatment and on days 1 and 8 posttreatment. **Arrowheads** indicate positively stained cells. Original magnification $\times$ 20. **B** and **C,** Endothelial cell apoptosis (as determined by the numbers of nuclei positive for cleaved caspase 3) (**B**) and proliferation (as determined by the numbers of nuclei positive for Ki-67) (**C**) in WT and transgenic mice before and after treatment with SU5416. Data were derived from 120 random fields at 20$\times$ magnification (n = 6 mice), comparing all time points. In **C,** cell counts were derived from only the medial and endothelial layers, to discount perivascular inflammatory cells. Values are the mean $\pm$ SEM. $* = P < 0.05$; $** = P < 0.01$; $*** = P < 0.001$. **D,** Representative images showing immunostaining for CD31 (red) and cleaved caspase 3 (green). **Arrowheads** indicate apoptotic endothelial cells, demonstrated by colocalization (yellow). Original magnification $\times$ 20. hpf = high-power field.

to avoid conflicting results due to the development of spontaneous lung fibrosis, which occurs in some TβRIIΔk-fib mice after age 16 weeks.

H&E staining showed widespread luminal cell proliferation with obliteration of some small and medium-sized vessels (Figure 4A). Overall, 39.7% of vessels were obliterated in transgenic mice, with none obliterated in the WT mice treated with SU5416 or vehicle alone, although minor degrees of cellular proliferation arising from the endothelium were seen in WT mice treated with SU5416 (Figure 4A). Sirius red staining revealed no exaggerated fibrosis in any group 21 days after SU5416 treatment, and CD31 immunostaining confirmed that the luminal cell proliferation observed in transgenic mice was derived from the endothelium (data not shown).

RVSP was elevated in transgenic mice following treatment with SU5416 (Figure 4B). Moreover, the RV mass index was also increased, suggesting RV hypertrophy in treated transgenic mice (Figure 4C). This confirms that the elevation in RVSP had hemodynamic significance not present constitutively in transgenic mice. VEGF inhibition in the TβRIIΔk-fib mouse strain consistently induced hemodynamically significant PAH, leading to RV hypertrophy.

Endothelial cell apoptosis and proliferation in the lungs following SU5416 treatment. To further investigate the mechanism for this PAH phenotype, we

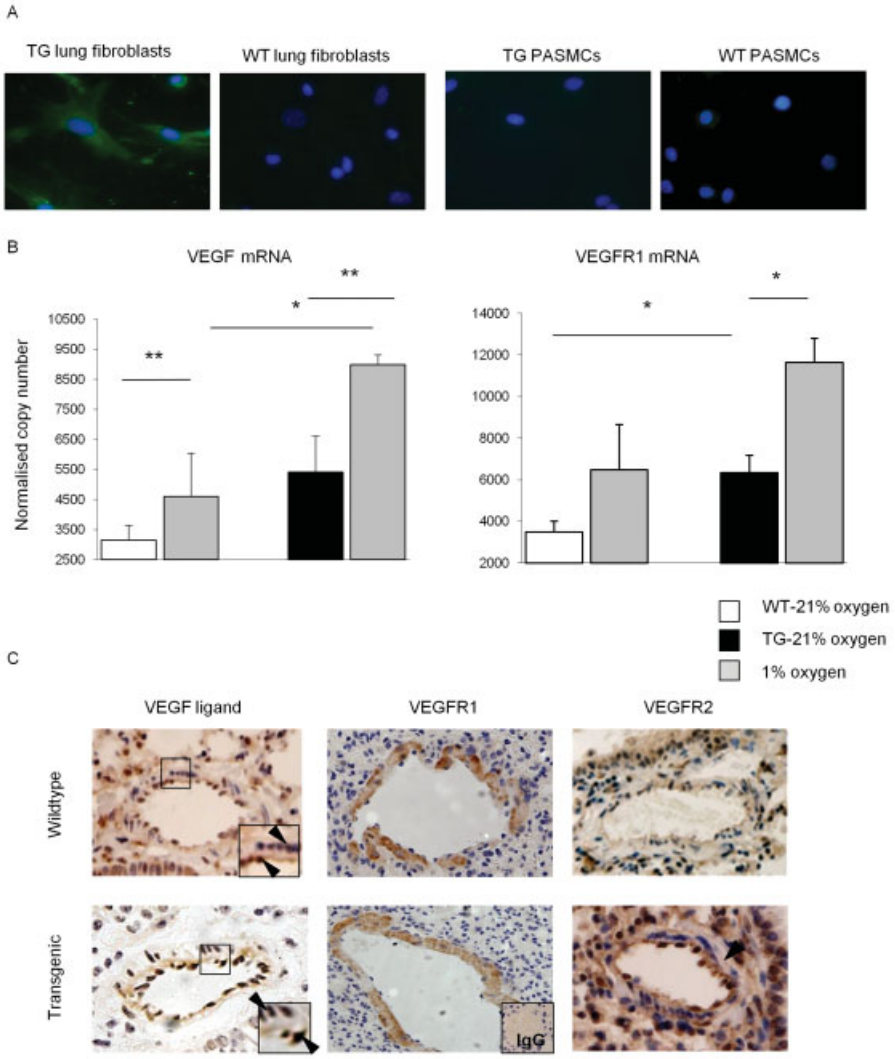

Figure 6. Gene expression patterns in pulmonary arterial smooth muscle cells (PASMCs) in response to hypoxia in the TβRIIΔk-fib mouse strain. **A,** Representative images showing β-galactosidase immunostaining of PASMCs and lung fibroblasts from wild-type (WT) and transgenic (TG) mice. Original magnification × 20. **B,** Expression of vascular endothelial growth factor (VEGF) and VEGF receptor 1 (VEGFR-1) mRNA in PASMCs. Bars show the mean ± SEM. $* = P < 0.05$; $** = P < 0.01$. **C,** Representative images showing immunostaining for VEGF ligand, VEGFR-1, and VEGFR-2 in pulmonary arterioles. **Insets,** Higher-magnification views of the boxed areas. **Arrowheads** indicate positive staining. Original magnification × 20.

examined cellular apoptosis (caspase 3 cleavage) and proliferation (Ki-67 staining) before and on day 1, day 8, and day 21 following SU5416 administration (Figures 5A–C). There was no apoptosis and little cell proliferation in the lungs of untreated adult WT mice, but transgenic mice expressed Ki-67 in the previously described perivascular infiltrates. After SU5416 administration, apoptosis occurred on day 1 in endothelial cells from both WT and transgenic mice and was not evident at other time points. On day 1 posttreatment, more cells stained for cleaved caspase 3 in the lung parenchyma of transgenic mice compared with the lung parenchyma of WT mice, perhaps reflecting capillary endothelial cell apoptosis in the lungs of the transgenic mice.

No difference in proliferation within the vessels was seen on day 1. Subsequently, proliferating endothelial cells were present in the vessels of transgenic mice (maximal on day 8), which is consistent with an exaggerated proliferative response to the initial apoptotic event. Endothelial cell proliferation was most clearly seen within the obliterative lesions of transgenic mice. These data are congruent with those from previous studies in

rat models and suggested that the vessel obliteration is attributable to apoptosis-resistant endothelial cell clones. Colocalization of cleaved caspase 3 and CD31 confirmed that endothelial cells were undergoing apoptosis in the pulmonary vessel walls of transgenic mice (Figure 5D).

Taken together, our data demonstrate that endothelial cell injury occurring in the context of perturbed vascular remodeling/repair due to altered TGFβ signaling in vascular adventitia and smooth muscle may trigger a phenotype reminiscent of PAH. The broader phenotype of the TβRIIΔk-fib mouse model and the results of earlier studies of epithelial injury and lung fibrosis are consistent with a central role of perturbed TGFβ signaling in fibroblasts as a pivotal pathogenic factor in the development of SSc-related complications, including PAH.

Gene expression patterns in TβRIIΔk-fib mouse PASMCs. The altered constitutive pulmonary vascular phenotype of the TβRIIΔk-fib mouse strain and exaggerated response to VEGFR-2 inhibition in the pulmonary arterial circulation led us to investigate gene expression responses in PASMCs, particularly responses to hypoxic stress, and whether these differed from the responses in vascular SMCs from other sites. PASMCs were cultured in hypoxic conditions and compared with aortic SMCs from the same mice and with PASMCs cultured under standard conditions.

First, β-galactosidase staining of PASMCs confirmed that they did not express the transgene (Figure 6A). More than 99% of cells expressed α-SMA, with no difference in expression or distribution between transgenic and WT mouse cells. Growth curves showed no significant differences (data not shown). Key gene expression differences in the VEGF signaling axis were present in the PASMCs from transgenic mice. Transgenic mouse PASMCs cultured in 21% oxygen expressed amounts of VEGF and VEGFR-1 similar to those expressed by WT mouse cells kept at 1% oxygen, and up-regulation of receptors in response to 1% oxygen was observed (Figure 6B). VEGFR-1 expression was 2-fold higher in transgenic mouse PASMCs than in aortic SMCs (mean $\pm$ SEM copy number 6,345 $\pm$ 836 versus 3,360 $\pm$ 289; $P < 0.01$), but the expression patterns in response to 1% oxygen and TGFβ were similar.

Figure 6C shows representative images of immunohistochemical staining for the expression of VEGF ligand and VEGFR. VEGF ligand expression within SMCs was up-regulated in transgenic mice. In WT mice, VEGF expression was confined to the endothelium. VEGFR-1 expression was present in the smooth muscle layer and was not increased in transgenic mice. VEGFR-2 expression was predominantly endothelial and was increased in transgenic mice. Thus, increased TGFβ activity in the pulmonary vasculature of transgenic mice results in up-regulated VEGF axis signaling, but this may confer a risk of increased susceptibility to endothelial cell apoptosis once VEGF axis signaling is temporarily inhibited by SU5416. The higher VEGF expression levels following inhibition in the transgenic mice may then be responsible for the exaggerated endothelial cell proliferation seen in the vessels of transgenic mice. Of interest, when exogenous TGFβ was administered to normal cultured human PASMCs, the effects on VEGF and VEGFR-1 expression were similar to those observed in transgenic mouse PASMCs (data not shown). This supports the underlying role of increased TGFβ activity in the transgenic mice and suggests that a similar mechanism could apply in human PASMCs.

DISCUSSION

In this study, we have added to earlier work evaluating a novel transgenic mouse model of scleroderma by defining, for the first time, the pulmonary vascular phenotype of the TβRIIΔk-fib mouse strain. Our findings provide fundamental insight into potential pathogenic mechanisms that are very relevant to human disease and especially to the development of SSc-associated PAH. In the TβRIIΔk-fib mouse strain, alterations in TGFβ and VEGF signaling within the pulmonary circulation were confirmed, together with a structural vasculopathy reminiscent of murine chronic hypoxic PH, with smooth muscle hypertrophy, inflammatory changes, and modest elevations in RV pressure. Furthermore, experimental pulmonary endothelial cell injury with an inhibitor of VEGF signaling induced obliterative endothelial proliferation and remodeling of the right ventricle. Our study provides compelling evidence for the role of altered TGFβ signaling in pulmonary vasculopathy and the importance of VEGF in endothelial cell homeostasis. This combination of genetic and pharmacologic perturbation is relevant to the pathogenesis of human SSc-related PAH.

The TβRIIΔk-fib mouse model has fibroblast-specific perturbation of TGFβ signaling: a kinase-deficient nonsignaling TGFβ receptor results in paradoxical excessive TGFβ signaling and a phenotype prone to fibrosis (17,18), with increased susceptibility to minor lung epithelial injury (21) and a systemic vasculopathy associated with a fibrotic left ventricular cardiomyopathy (22). The observation that fibroblast-specific transgene expression results in an activated phenotype in epithe-

lium and SMCs is testament to the likelihood of bystander effects on other cell types and a key regulatory and homeostatic role for resident fibroblasts. Up-regulation of VEGF ligand and VEGFR is likely to lead to increased VEGF axis activity in vivo, which may underlie some of the changes in the vascular SMC layer seen in both the transgenic mice and the WT hypoxic mice. In this study, we demonstrate that TGFβ1 up-regulates VEGF signaling in human PASMCs, which is consistent with previous reports (24–26).

We propose that up-regulated VEGF signaling in transgenic mice becomes a critical factor for pulmonary endothelial cell homeostasis and survival and reflects detrimental effects of increased TGFβ exposure on vascular endothelial cells and SMCs (27). Our in vitro experiments show up-regulated VEGF signaling in PASMCs compared with aortic SMCs from transgenic mice, but in vivo experiments are not directly comparable with the situation in vivo, where PASMCs subsist in an environment with lower oxygen concentrations than those in which aortic SMCs subsist.

Similar to what occurs in the chronic hypoxia model, increased activity of the VEGF ligand/receptor axis may render pulmonary arterial endothelial cells from transgenic mice more susceptible than those from WT mice to the effects of SU5416. Paradoxically, up-regulated VEGF signaling also leads to enhanced proliferation and reduced apoptosis of endothelial cells and underlies the exaggerated intimal and luminal changes seen after SU5416 exposure. This severe obliterative vascular disease is reminiscent of SSc-related PAH. A key strength of our model is that it obviates the need for long-term exposure to hypoxia in generating a PAH-like pathology, although both this and the chronic hypoxia model could be considered an extreme phenotype in comparison with the human disease. Potential interplay between the constitutive fibroblast-dependent up-regulation of TGFβ activity, increased VEGF ligand and receptor expression, and the impact of transient SU5416-mediated pharmacologic inhibition of VEGFR-2 leads to the development of a PAH-like phenotype in this transgenic mouse strain.

It is probable that changes in the vascular tree within the lungs of patients with SSc-related PAH reflect an aberrant fibrotic response to a vascular insult. Dysfunctional myocardial adaptive responses to pressure overload of the right ventricle due to subclinical inflammatory and fibrotic myocardial disease may also contribute to the clinical picture (28,29). Furthermore, when pulmonary fibrosis coexists, the contribution to symptoms and pulmonary pressure must not be understated. At 16 weeks of age, 25% of TβRIIΔk-fib mice develop spontaneous mild pulmonary fibrosis, and although younger mice were used in this study (to avoid this confounder), the propensity for pulmonary fibrosis and fibrotic ventricular change in this model (18,22) does reflect this clinical situation. Thus, the investigation of older TβRIIΔk-fib mice would be relevant to investigate the interplay of lung fibrosis, PAH, and fibrotic myocardial disease.

When characterizing SSc-related PAH in particular, there are some important considerations. Veno-occlusive disease has been reported more frequently in SSc-related PAH than in idiopathic PAH (12,13), although there is no evidence of venous involvement in the TβRIIΔk-fib mouse model. The relative role of inflammation in the pathogenesis of SSc-related PAH when compared with idiopathic PAH is also relevant. There is perivascular inflammation in both idiopathic PAH and SSc-related PAH, and detailed characterization of these inflammatory infiltrates in patients with idiopathic PAH was recently described (30). Gene expression analyses have identified inflammatory signatures in both idiopathic PAH and SSc-related PAH (31). SSc-related PAH has been labeled a prototypic inflammatory disease due to the autoantibody associations and identification of early inflammatory cell recruitment (7), but the precise role of inflammation in the pathogenesis of either condition remains unclear.

The contribution of endothelial cells to the pathogenesis of PAH is uncertain but highly relevant to this study. Data supporting a role for endothelial cell perturbation in SSc-associated vasculopathy and PAH in vivo are available from several studies, but information regarding direct functional mechanisms is lacking. It is likely that healthy endothelial cells interact with SMCs and fibroblasts for vessel homeostasis, and it is plausible that VEGF-mediated pathways modulate endothelial cell responses to hypoxia.

Both vascular pathology and fibrosis have been described in genetic mouse models of SSc. Caveolin 1–knockout mice were shown to have high TGFβ bioactivity, with abnormal endothelial function and increased RV pressure without the cardinal features of PAH (32). The Fra-2–transgenic mouse strain has altered activated protein 1 signaling and severe fibrosis of the lung and kidney, resulting in early mortality. Ubiquitous transgene expression and an inability to distinguish endogenous from transgenic expression of Fra-2 complicate analysis of the mechanism of fibrosis and vasculopathy, although the model has clear relevance to cases of SSc in which lung fibrosis and PH coexist (33)

and a predominant fibrotic phenotype. A major strength of the present study is the use of a model that clearly reflects the likely pathogenetic mechanism underlying SSc-associated vascular disease and the potential to aggravate the phenotype with a relevant trigger. Aberrant TGFβ signaling is widely recognized to be related to SSc pathogenesis, and this model provides a plausible mechanism for the secondary alterations in related signaling pathways resulting in the development of vasculopathy.

In conclusion, in this study we replicated features of human SSc-related PAH in a relevant transgenic mouse model and defined likely pathogenic mechanisms underlying this novel phenotype. Thus, we suggest a paradigm in which a background TGFβ-dependent pulmonary vasculopathy renders mice susceptible to endothelial cell proliferation after injury, leading to hallmark features of SSc-related PAH. In addition to providing mechanistic insights, this model also provides a platform for preclinical interventional studies of this important complication of SSc and for exploration of potential treatment strategies that attenuate other mediators or signaling pathways that might be regulated by TGFβ or VEGF.

AUTHOR CONTRIBUTIONS

All authors were involved in drafting the article or revising it critically for important intellectual content, and all authors approved the final version to be published. Dr. Denton had full access to all of the data in the study and takes responsibility for the integrity of the data and the accuracy of the data analysis.

Study conception and design. Derrett-Smith, Khan, Baliga, Holmes, Abraham, Denton.

Acquisition of data. Derrett-Smith, Dooley, Gilbane, Trinder, Khan, Baliga, Hobbs, Denton.

Analysis and interpretation of data. Derrett-Smith, Khan, Baliga, Abraham, Denton.

REFERENCES

1. Hachulla E, Coghlan JG. A new era in the management of pulmonary arterial hypertension related to scleroderma: endothelin receptor antagonism [review]. Ann Rheum Dis 2004;63: 1009–14.
2. Avouac J, Airo P, Meune C, Beretta L, Dieude P, Caramaschi P, et al. Prevalence of pulmonary hypertension in systemic sclerosis in European Caucasians and meta-analysis of 5 studies. J Rheumatol 2010; 37:2290–8.
3. Fisher MR, Mathai SC, Champion HC, Girgis RE, Houston-Harris T, Hummers L, et al. Clinical differences between idiopathic and scleroderma-related pulmonary hypertension. Arthritis Rheum 2006;54:3043–50.
4. Tan FK. Systemic sclerosis: the susceptible host (genetics and environment) [review]. Rheum Dis Clin North Am 2003;29: 211–37.
5. Jonigk D, Golpon H, Bockmeyer CL, Maegel L, Hoeper MM, Gottlieb J, et al. Plexiform lesions in pulmonary arterial hypertension: composition, architecture, and microenvironment. Am J Pathol 2011;179:167–79.
6. Al Sabbagh MR, Steen VD, Zee BC, Nalesnik M, Trostle DC, Bedetti CD, et al. Pulmonary arterial histology and morphometry in systemic sclerosis: a case-control autopsy study. J Rheumatol 1989;16:1038–42.
7. Hassoun PM, Mouthon L, Barbera JA, Eddahibi S, Flores SC, Grimminger F, et al. Inflammation, growth factors and pulmonary vascular remodeling. J Am Coll Cardiol 2009;54:S10–9.
8. Okawa-Takatsuji M, Aotsuka S, Fujinami M, Uwatoko S, Kinoshita M, Sumiya M. Up-regulation of intercellular adhesion molecule-1 (ICAM-1), endothelial leucocyte adhesion molecule-1 (ELAM-1) and class II MHC molecules on pulmonary artery endothelial cells by antibodies against U1-ribonucleoprotein. Clin Exp Immunol 1999;116:174–80.
9. Lee SD, Shroyer KR, Markham NE, Cool CD, Voelkel NF, Tuder RM. Monoclonal endothelial cell proliferation is present in primary but not secondary pulmonary hypertension. J Clin Invest 1998;101:927–34.
10. Choi JJ, Min DJ, Cho ML, Min SY, Kim SJ, Lee SS, et al. Elevated vascular endothelial growth factor in systemic sclerosis. J Rheumatol 2003;30:1529–33.
11. Distler O, Del Rosso A, Giacomelli R, Cipriani P, Conforti ML, Guiducci S, et al. Angiogenic and angiostatic factors in systemic sclerosis: increased levels of vascular endothelial growth factor are a feature of the earliest disease stages and are associated with the absence of fingertip ulcers. Arthritis Res 2002;4:R11.
12. Dorfmuller P, Humbert M, Perros F, Sanchez O, Simonneau G, Muller KM, et al. Fibrous remodeling of the pulmonary venous system in pulmonary arterial hypertension associated with connective tissue diseases. Hum Pathol 2007;38:893–902.
13. Overbeek MJ, Vonk MC, Boonstra A, Voskuyl AE, Vonk-Noordegraaf A, Smit EF, et al. Pulmonary arterial hypertension in limited cutaneous systemic sclerosis: a distinctive vasculopathy. Eur Respir J 2009;34:371–9.
14. Tew MB, Arnett FC, Reveille JD, Tan FK. Mutations of bone morphogenetic protein receptor type II are not found in patients with pulmonary hypertension and underlying connective tissue diseases [letter]. Arthritis Rheum 2002;46:2829–30.
15. Wipff J, Kahan A, Hachulla E, Sibilia J, Cabane J, Meyer O, et al. Association between an endoglin gene polymorphism and systemic sclerosis-related pulmonary arterial hypertension. Rheumatology (Oxford) 2007;46:622–5.
16. Wipff J, Dieude P, Guedj M, Ruiz B, Riemekasten G, Cracowski JL, et al. Association of a KCNA5 gene polymorphism with systemic sclerosis–associated pulmonary arterial hypertension in the European Caucasian population. Arthritis Rheum 2010;62: 3093–100.
17. Denton CP, Zheng B, Evans LA, Shi-wen X, Ong VH, Fisher I, et al. Fibroblast-specific expression of a kinase-deficient type II transforming growth factor β receptor leads to paradoxical activation of TGF β signaling pathways with fibrosis in transgenic mice. J Biol Chem 2003;278:25109–19.
18. Denton CP, Lindahl GE, Khan K, Shiwen X, Ong VH, Gaspar NJ, et al. Activation of key profibrotic mechanisms in transgenic fibroblasts expressing kinase-deficient type II transforming growth factor-β receptor (TβRIIΔk). J Biol Chem 2005;280:16053–65.
19. Taraseviciene-Stewart L, Kasahara Y, Alger L, Hirth P, McMahon G, Waltenberger J, et al. Inhibition of the VEGF receptor 2 combined with chronic hypoxia causes cell death-dependent pulmonary endothelial cell proliferation and severe pulmonary hypertension. FASEB J 2001;15:427–38.
20. Ciuclan L, Bonneau O, Hussey M, Duggan N, Holmes AM, Good R, et al. A novel murine model of severe pulmonary arterial hypertension. Am J Respir Crit Care Med 2011;184:1171–82.
21. Hoyles RK, Khan K, Shiwen X, Howat SL, Lindahl GE, Leoni P, et al. Fibroblast-specific perturbation of transforming growth

factor β signaling provides insight into potential pathogenic mechanisms of scleroderma-associated lung fibrosis: exaggerated response to alveolar epithelial injury in a novel mouse model. Arthritis Rheum 2008;58:1175–88.
22. Derrett-Smith EC, Dooley A, Khan K, Shi-wen X, Abraham D, Denton CP. Systemic vasculopathy with altered vasoreactivity in a transgenic mouse model of scleroderma. Arthritis Res Ther 2010; 12:R69.
23. Vandesompele J, De Preter K, Pattyn F, Poppe B, Van Roy N, De Paepe A, et al. Accurate normalization of real-time quantitative RT-PCR data by geometric averaging of multiple internal control genes. Genome Biology 2002;3:1–11.
24. Tanabe K, Tokuda H, Takai S, Matsushima-Nishiwaki R, Hanai Y, Hirade K, et al. Modulation by the steroid/thyroid hormone superfamily of TGF-β-stimulated VEGF release from vascular smooth muscle cells. J Cell Biochem 2006;99:187–95.
25. Mata-Greenwood E, Grobe A, Kumar S, Noskina Y, Black SM. Cyclic stretch increases VEGF expression in pulmonary arterial smooth muscle cells via TGF-β1 and reactive oxygen species: a requirement for NAD(P)H oxidase. Am J Physiol Lung Cell Mol Physiol 2005;289:L288–98.
26. Kobayashi T, Liu X, Wen FQ, Fang Q, Abe S, Wang XQ, et al. Smad3 mediates TGF-β1 induction of VEGF production in lung fibroblasts. Biochem Biophys Res Commun 2005;327:393–8.
27. Ferrari G, Terushkin V, Wolff MJ, Zhang X, Valacca C, Poggio P, et al. TGF-β1 induces endothelial cell apoptosis by shifting VEGF activation of p38MAPK from the prosurvival p38β to proapoptotic p38α. Mol Cancer Res 2012;10:605–14.
28. Fernandes F, Ramires FJ, Arteaga E, Ianni BM, Bonfa ES, Mady C. Cardiac remodeling in patients with systemic sclerosis with no signs or symptoms of heart failure: an endomyocardial biopsy study. J Card Fail 2003;9:311–7.
29. Overbeek MJ, Lankhaar JW, Westerhof N, Voskuyl AE, Boonstra A, Bronzwaer JG, et al. Right ventricular contractility in systemic sclerosis-associated and idiopathic pulmonary arterial hypertension. Eur Respir J 2008;31:1160–6.
30. Grigoryev DN, Mathai SC, Fisher MR, Girgis RE, Zaiman AL, Housten-Harris T, et al. Identification of candidate genes in scleroderma-related pulmonary arterial hypertension. Transl Res 2008;151:197–207.
31. Savai R, Pullamsetti SS, Kolbe J, Bieniek E, Voswinckel R, Fink L, et al. Immune and inflammatory cell involvement in the pathology of idiopathic pulmonary arterial hypertension. Am J Respir Crit Care Med 2012;186:897–90.
32. Razani B, Engelman JA, Wang XB, Schubert W, Zhang XL, Marks CB, et al. Caveolin-1 null mice are viable but show evidence of hyperproliferative and vascular abnormalities. J Biol Chem 2001;276:38121–38.
33. Maurer B, Reich N, Juengel A, Kriegsmann J, Gay RE, Schett G, et al. Fra-2 transgenic mice as a novel model of pulmonary hypertension associated with systemic sclerosis. Ann Rheum Dis 2012;71:1382–7.